

Electron Bernstein Wave Excitation in NSTX-Type High- β Plasmas¹

Abhay K. Ram²

*Plasma Science and Fusion Center
Massachusetts Institute of Technology
Cambridge, Massachusetts 02139. U.S.A.*

INTRODUCTION

There are distinct advantages to using radio-frequency waves in the electron cyclotron range of frequencies (ECRF) for heating fusion plasmas and for driving plasma currents. These advantages include the ease in coupling EC power into the plasmas and the ability to readily adjust the launch angles. The major drawback, as far as conventional fusion tokamaks are concerned, is the unavailability of cw sources at very high frequencies (above the electron plasma frequency). For spherical tokamaks, like the National Spherical Tokamak Experiment (NSTX) where $f_{pe}/f_{ce} \gg 1$ (f_{pe} and f_{ce} are the electron plasma and cyclotron frequencies, respectively) in the core of the plasma, the problem is even more acute. In order to access the core of the plasma the ratio of the wave frequency f to f_{ce} has to be much greater than one. Otherwise, the externally launched O-mode and/or X-mode would be cutoff right near the plasma edge. For $f > f_{pe} \gg f_{ce}$ the damping of the O-mode or the X-mode at high harmonics of the electron cyclotron frequency is weak. A possible mechanism for by-passing these problems is to mode convert the from the X-mode to the electron Bernstein wave (EBW) at the upper-hybrid resonance (UHR). The EBW has no density limit, propagates for frequencies above f_{ce} , and is damped on electrons near the Doppler-shifted electron cyclotron resonance or its harmonics. There are two techniques for coupling power to EBWs. The first technique is to launch the fast X-mode from the outboard side [1-4]. The fast X-mode tunnels through the upper hybrid resonance and couples to the slow X-mode, which, in turn, mode converts to EBWs at the upper-hybrid resonance. This is referred to as the FX-B mode conversion process. This process involves, in the cold plasma limit, the fast X-mode right-hand cutoff, the UHR, and the left-hand cutoff of the slow X-mode. Recently, in a different, low frequency, context we have obtained an analytical solution to a model full-wave differential equation containing such a triplet [5,6]. Using this analytical model we have studied the

¹) Work supported by Department of Energy and NSTX

²) In collaboration with Abraham Bers and Steven D. Schultz, M.I.T.

FX-B mode conversion process [2]. The second technique involves the launching of an O-mode, from the outboard side, at such an angle (relative to the magnetic field) that the O-mode cutoff is spatially located at the same point as the left-hand cutoff of the slow X-mode [7-10]. Then the O-mode power is coupled to the slow X-mode, which in turn mode converts to EBWs at the upper-hybrid resonance. This technique is referred to as the O-SX-B mode conversion process.

The FX-B and the O-SX-B mode conversion processes have also been studied using numerical integration of the full wave differential equations [3]. We find that the two mode conversion processes are optimized in different regimes of frequency and parallel wavelength parameter space.

ANALYTICAL MODELLING OF FX-B MODE CONVERSION

Assuming a cold plasma with an equilibrium magnetic field $\vec{B} = B_0 \hat{z}$ in the toroidal direction only, and considering a slab geometry model for the radial (x-direction) propagation of only extraordinary waves in the equatorial plane, the poloidal (y-direction) component of the wave electric field is given by

$$\frac{d^2 E_y}{dx^2} + \frac{\omega^2}{c^2} \frac{K_R K_L}{K_\perp} E_y = 0 \quad (1)$$

where we have assumed a cold plasma with

$$K_R = \frac{\omega(\omega - \omega_{ce}) - \omega_{pe}^2}{\omega(\omega - \omega_{ce})} \equiv \frac{(\omega - \omega_R)(\omega + \omega_L)}{\omega(\omega - \omega_{ce})} \quad (2)$$

$$K_L = \frac{\omega(\omega + \omega_{ce}) - \omega_{pe}^2}{\omega(\omega + \omega_{ce})} \equiv \frac{(\omega - \omega_L)(\omega + \omega_R)}{\omega(\omega + \omega_{ce})} \quad (3)$$

$$K_\perp = \frac{\omega^2 - (\omega_{pe}^2 + \omega_{ce}^2)}{\omega^2 - \omega_{ce}^2} \equiv \frac{\omega^2 - \omega_{UH}^2}{\omega^2 - \omega_{ce}^2} \quad (4)$$

ω is the angular frequency of the wave, c is the speed of light, $\omega_{pe}(x)$ and $\omega_{ce}(x)$ are the electron plasma and cyclotron frequencies, respectively. Equation (1) describes the propagation of the X-mode through a resonance ($K_\perp = 0$), and the right-hand ($K_R = 0$) and left-hand ($K_L = 0$) cutoffs. This wave equation can be solved analytically, by expanding the x-dependence of (2)-(4) in the vicinity of the UHR, as we have shown before [2]. We find that for an incident X-mode from the low B-field side, the fraction of incident power that is resonantly absorbed at the UHR (hence, mode converted to EBWs) is given by

$$C = 4e^{-\pi\eta} (1 - e^{-\pi\eta}) \cos^2 \left(\frac{\phi}{2} + \theta \right) \quad (5)$$

as previously shown for a similar problem [5,6]; here θ is the phase of the Gamma function $\Gamma(-i\eta/2)$, ϕ is essentially the phase of the wave reflected from the SX left-hand cutoff relative to the incident SX wave, and η is the Budden parameter [11] given by [2]

$$\eta = \frac{\omega_{ce}(x = x_{UHR})}{\sqrt{2}c} L_n, \text{ where } L_n = \left| \frac{d}{dx} \ln n_0(x) \right|_{x=x_{UHR}}^{-1}. \quad (6)$$

From (5), it is clear that $C = 1$, i.e., 100% of the incident X-mode power is resonantly absorbed (mode converted to EBW), provided $(\theta + \phi/2) = (2n + 1)\pi/2$, for n any integer, and $\exp(-\pi\eta) = 0.5$ or, equivalently, $\eta \approx 0.22$. From (6) we note that that $C = 1$ if $|BL_n|_{UHR} \approx 5.3 \times 10^{-4}$ T m, where B is the toroidal magnetic field in Teslas at the UHR and L_n is in meters. For low magnetic fields we require a steep density gradient which can be realized near the edge of the plasma.

NUMERICAL INTEGRATIONS OF THE FULL-WAVE EQUATIONS

We have developed two numerical codes that solve for the mode conversion coefficient in an inhomogeneous slab plasma with a sheared magnetic field. Since the codes allow for arbitrary k_{\parallel} , the X-mode and the O-mode can no longer be distinctly identified. The first code uses the cold plasma model in which the resonance absorption at the UHR gives the mode conversion coefficient. This is a fourth order ordinary differential equation. The second code uses an approximate kinetic (Maxwellian) plasma model in which the EBW can be clearly identified. This is a sixth order ordinary differential equation and the mode conversion coefficient is determined from the actual power flowing in EBW. Below we outline the cold plasma model and the approximate kinetic mode conversion model. The details of these models can be found in [3,4]. We will show a comparison between the results from the cold plasma model and the approximate kinetic plasma model, and the analytic results of the simpler model given in Section II.

Cold Plasma Model

In the high frequency regimes of interest the ion dynamics can be ignored. From the electron fluid equations and Maxwell's equations we find that the first order electric and magnetic fields are given by

$$\nabla \times \vec{E}_1 = i\omega \vec{B}_1, \quad \nabla \times \vec{B}_1 = -i\frac{\omega}{c^2} \vec{K} \cdot \vec{E}_1 \quad (7)$$

where $\vec{K}(x, \omega) = \vec{I} + \vec{\chi}$ is the permittivity tensor, and

$$\vec{\chi} = \frac{-\alpha^2}{(1-\beta^2)} \begin{pmatrix} 1 & -i\beta \cos(\Psi) & i\beta \sin(\Psi) \\ i\beta \cos(\Psi) & 1 - \beta^2 \sin(\Psi)^2 & -\beta^2 \sin(\Psi) \cos(\Psi) \\ -i\beta \sin(\Psi) & -\beta^2 \sin(\Psi) \cos(\Psi) & 1 - \beta^2 \cos(\Psi)^2 \end{pmatrix} \quad (8)$$

is the susceptibility tensor with

$$\alpha^2 = \frac{\omega_p^2(x)}{\omega^2} ; \quad \omega_p^2 = \frac{e^2 n_0(x)}{m_e \epsilon_0} ; \quad \beta = \frac{\omega_c(x)}{\omega} ; \quad \omega_c = \frac{e B_0(x)}{m_e} \quad (9)$$

and $\Psi = \Psi(x)$ is the angle between the direction of the total magnetic field \vec{B}_0 and the z-axis.

Assuming that the plasma is uniform in the y and z directions, we can Fourier analyze in these directions and obtain, from (7), the following equations for the spatial evolution of the wave fields:

$$\frac{d\vec{F}_c}{d\xi} = i\vec{A}_c \cdot \vec{F}_c \quad (10)$$

where $\xi = (\omega x/c)$, the transpose of \vec{F}_c is $\vec{F}_c^* = (E_y, E_z, -cB_y, cB_z)$, and

$$\vec{A}_c = \frac{1}{K_{xx}} \begin{bmatrix} -n_y \chi_{xy} & -n_y \chi_{xz} & -n_y n_z & K_{xx} - n_y^2 \\ -n_z \chi_{xy} & -n_z \chi_{xz} & K_{xx} - n_z^2 & -n_y n_z \\ K_{xx}(\chi_{yz} + n_y n_z) & K_{xx}(K_{zz} - n_y^2) & n_z \chi_{xz} & n_y \chi_{xz} \\ +\chi_{xy} \chi_{xz} & +\chi_{xz}^2 & & \\ K_{xx}(K_{yy} - n_z^2) & K_{xx}(\chi_{yz} + n_y n_z) & n_z \chi_{xy} & n_y \chi_{xy} \\ +\chi_{xy}^2 & +\chi_{xy} \chi_{xz} & & \end{bmatrix} \quad (11)$$

Here $k_y = (\omega n_y/c)$ and $k_z = (\omega n_z/c)$ are the wavevector components in the y and z directions, respectively. The cold plasma permittivity and susceptibility tensors in the sheared magnetic field are readily obtained from the usual ones given in standard plasma texts [12].

Kinetic Modelling to Include the EBW

We have also developed a formulation that includes the kinetic electron-Bernstein wave (EBW) and the cold plasma modes. In a homogeneous plasma, the electrostatic EBW is associated with the K_{xx} component of the kinetic (Vlasov) permittivity tensor [13]. For weak damping and in the frequency regime between the first and the second electron cyclotron harmonics, it is sufficient to expand the kinetic

susceptibility χ_{xx}^K to second order in $(k_\perp v_T/\omega_{ce})$ where $v_{Te}^2 = (\kappa T_e/m_e)$. We find that for a Maxwellian electron distribution function

$$\chi_{xx}^K \approx \chi_{xx} + T n_x^2 \quad (12)$$

where χ_{xx} is the cold plasma susceptibility, $n_x = (ck_x/\omega)$, and

$$T = \frac{-3\omega_{pe}^2 \omega^2 (v_{Te}/c)^2}{(\omega^2 - \omega_{ce}^2)(\omega^2 - 4\omega_{ce}^2)} \quad (13)$$

Assuming that $\chi_{xx}^K(x)$ is a slowly varying function of x , the conservation of the kinetic energy flow density [14] in x requires that we do the following transformation in the cold plasma x-component of the electric displacement field [15]:

$$K_{xx}E_x \rightarrow K_{xx}E_x - \frac{d}{d\xi} \left(T \frac{dE_x}{d\xi} \right) \quad (14)$$

Then, from Maxwell's equations, the spatial evolution of the wave fields is given by:

$$\frac{d\vec{F}_K}{d\xi} = i\vec{A}_K^\leftrightarrow \cdot \vec{F}_K, \quad (15)$$

where the transpose of \vec{F}_K is $\vec{F}_K^* = [E_x, E_y, E_z, (iT E'_x), cB_z, -cB_y]$, $E'_x = (dE_x/d\xi)$, and

$$\vec{A}_K^\leftrightarrow = \begin{bmatrix} 0 & 0 & 0 & -T^{-1} & 0 & 0 \\ n_y & 0 & 0 & 0 & 1 & 0 \\ n_z & 0 & 0 & 0 & 0 & 1 \\ K_{xx} & \chi_{xy} & \chi_{xz} & 0 & n_y & n_z \\ -\chi_{xy} & K_{yy} - n_z^2 & \chi_{yz} + n_y n_z & 0 & 0 & 0 \\ -\chi_{xz} & \chi_{yz} + n_y n_z & K_{zz} - n_y^2 & 0 & 0 & 0 \end{bmatrix}. \quad (16)$$

The kinetic power mode converted to EBWs is then obtained from integrating (15) with the appropriate boundary conditions.

Numerical Integration Results

We have carried out numerical integrations of (10) and (15) for a high- β NSTX-type equilibrium [16] for evaluating the X-B mode conversion efficiency as a function of the incident wave frequency. We assume that the (Shafranov shifted) minor radius is $a = 0.44$ m, the major radius is $R = 1.05$ m, the peak electron density is $n_{e0} = 3 \times 10^{19} \text{ m}^{-3}$, the density profile is $n_e/n_{e0} = (1 - n_E)(1 - x^2/a^2)^{1/2} + n_E$ where $n_E = 0.02$ and x is the distance along the equatorial plane ($x = 0$ being the center of the plasma column), the peak plasma temperature is $T_0 = 3$ keV, the

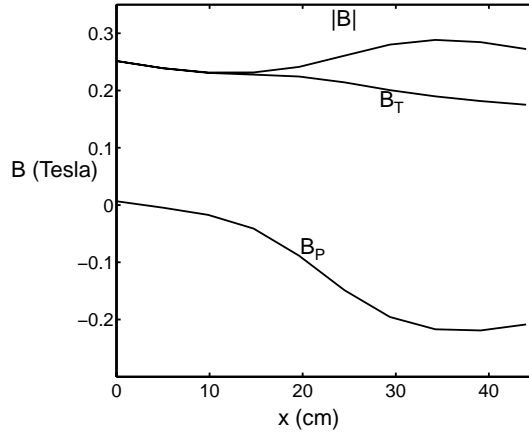


FIGURE 1. The magnetic field profile along the equatorial plane for a high- β NSTX scenario. B_T , B_P , and $|B|$ are the toroidal component, poloidal component, and magnitude of the magnetic field.

temperature profile is $T_e/T_0 = (1 - T_E)(1 - x^2/a^2)^2 + T_E$ with $T_E = 0.02$, and the magnetic field profile is as shown in Fig. 1. In Fig. 2(a) we plot the results for mode conversion coefficient as a function of the wave frequency for different models. The solid line is the theoretically obtained maximum mode conversion coefficient from (5):

$$C_{max} = 4e^{-\pi\eta} (1 - e^{-\pi\eta}) \quad (17)$$

The agreement between the results obtained from the two approaches to numerical integrations is remarkable. This demonstrates that the cold plasma resonant absorption model gives a good estimate of the fraction of the incident power that will be mode converted to EBWs. Furthermore, the theoretically obtained maximum mode conversion coefficient also gives a good estimate of the power mode converted to EBWs for NSTX.

Figure 2(b) shows the FX-B mode conversion coefficient as a function of n_z for a fixed source frequency of 15 GHz. This shows that the FX-B mode conversion process is most effective for $n_z \approx 0$. In comparison, for the same NSTX equilibrium plasma parameters, Fig. 3 shows that the O-X-B mode conversion process is most effective for a source frequency of 28 GHz and $n_z \approx 0.48$. Thus, the optimum X-B and O-X-B mode conversion processes tend to occur in different regions of the frequency and parallel wavelength parameter space. In addition, near the optimum mode conversion, the O-X-B mode conversion drops-off more rapidly with n_z than the FX-B mode conversion.

We have recently followed the EBW ray trajectories for model NSTX profiles using a general ray tracing package [17]. The ray trajectories are obtained in a fully kinetic (Maxwellian), non-relativistic, plasma. We find that the EBW damps locally at the Doppler-shifted electron cyclotron resonance or its harmonics. The

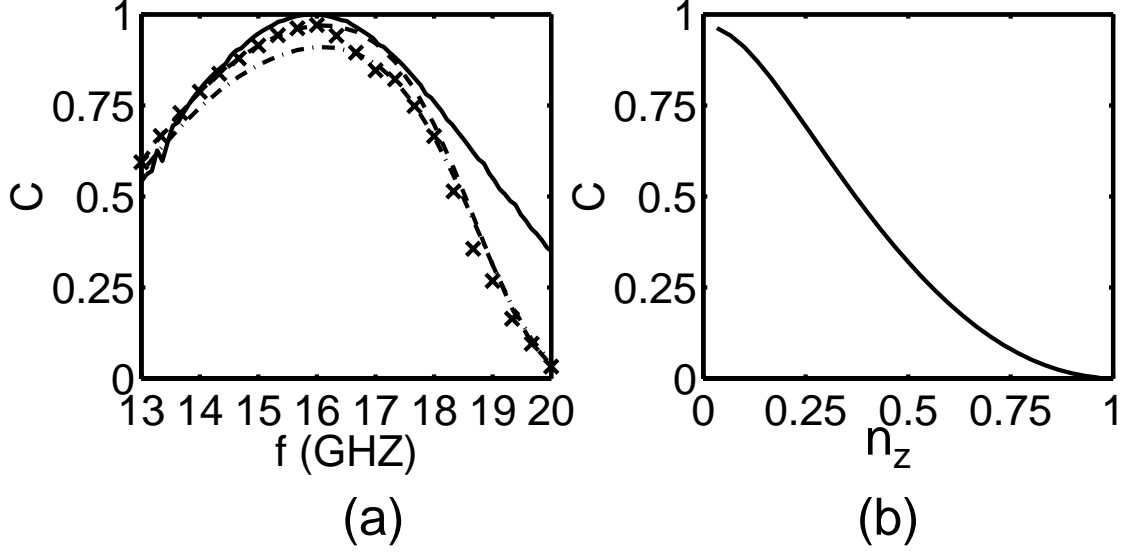


FIGURE 2. (a): The FX-B power mode conversion coefficient as a function of the wave frequency for NSTX-type parameters. Cold plasma model (10): $n_z = 0$ (dashed line), $n_z = 0.1$ (dashed-dotted line). Kinetic mode (15): $n_z = 0$ (crosses). Theoretical maximum (17): $n_z = 0$ (solid line); (b): The FX-B power mode conversion coefficient as a function of n_z as obtained from the numerical integration of the cold plasma model (10) for a wave frequency of 15 GHz.

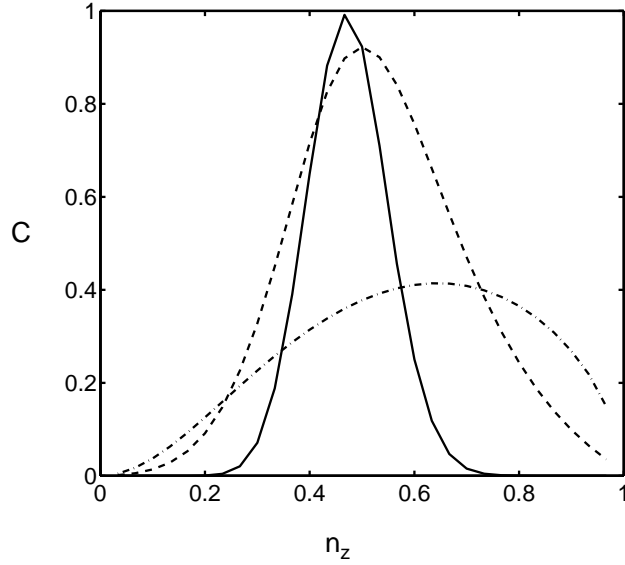


FIGURE 3. The O-X-B power mode conversion coefficient, from numerical integration of the cold plasma model (10), as a function of n_z ($n_y = 0$) for three different wave frequencies. The solid, dashed, and dashed-dotted lines are for wave frequencies of 28 GHz, 21 GHz, and 14 GHz, respectively.

k_{\parallel} along the ray trajectories vary over a large range if the rays are launched off the equatorial plane. This is due to the effect of a significant poloidal magnetic field [17]. The large k_{\parallel} 's lead to an appreciable Doppler shift from the actual electron cyclotron resonance (or its harmonics) so that the damping could be far removed from the electron cyclotron resonance layer. In spite of the large increases in k_{\parallel} the damping on electrons is still due to the Doppler-shifted cyclotron resonance rather than Landau damping. The plasma region in which the damping of the EBW is desired, either for heating or for driving plasma currents, can be controlled by an appropriate launching angle in the poloidal plane. These results will be discussed in a future publication.

REFERENCES

1. Nakajima S., and Abe, H., *Phys. Rev. A* **38**, 4373 (1988).
2. Wu, K. C., Ram, A. K., Bers, A., and Schultz, S. D., in *Proceedings of the 12th Topical Conference on RF Power in Plasmas*, eds. P. M. Ryan and T. Intrator, AIP Conference Proceedings 403, AIP, New York, 1997, pp. 207–210.
3. Bers, A., Ram, A. K., and Schultz, S. D., in *Proceedings of the Second Europhysics Topical Conference on RF Heating and Current Drive of Fusion Devices*, Brussels, Belgium, January 20–23, 1998, eds. J. Jacquinot, G. Van Oost, and R. R. Weynants (Contributed Papers, European Physical Society, Vol. 22A, Petit-Lancy, Switzerland), pp. 237–240 (1998).
4. Schultz, S. D., Ram, A. K., and Bers, A., paper IAEA-F1-CN-69/CDP/13, to appear in *Proceedings of the 17th International Atomic Energy Agency Fusion Energy Conference*, Yokohama, Japan, October 19–24, 1998.
5. Fuchs, V., Ram, A. K., Schultz, S. D., Bers, A., and Lashmore-Davies, C. N., *Phys. Plas.* **2**, 1637 (1995).
6. Ram, A. K., Bers, A., Schultz, S. D., and Fuchs, V., *Phys. Plas.* **3**, 1976 (1996).
7. Preinhaelter, J., and Kopecky, V., *J. Plas. Phys.* **10**, 1 (1973).
8. Weitzner, H., and Batchelor, D. B., *Phys. Fluids* **22**, 1355 (1979).
9. Nakajima, S., and Abe, H., *Phys. Lett. A* **124**, 295 (1987).
10. Hansen, F. R., Lynov, J. P., Mardi, C., Petrillo, V., *J. Plas. Phys.* **39**, 319 (1988).
11. Budden, K., *The Propagation of Radio Waves*, Cambridge University Press, 1985, pp. 596–602.
12. See, for example, Allis, W. P., Buchsbaum, S. J., and Bers, A., *Waves in Anisotropic Plasmas*, M.I.T. Press, Cambridge, 1963, Chapter 2; and Stix, T., *Waves in Plasmas*, A.I.P., New York, 1992, pp. 74–78.
13. See, for example, Chapter 11 in the last reference in [12].
14. Bers, A., in *Plasma Physics — Les Houches 1972* (eds. C. DeWitt and J. Peyraud), Gordon and Breach, New York, 1975, pp. 126–137.
15. Berk, H., and Book, D. L., *Phys. Fluids*, **12**, 649 (1969).
16. Plasma equilibrium and B-field profiles provided by Dr. R. Majeski of the Princeton Plasma Physics Laboratory.
17. Ram, A. K., and Bers, A., *Phys. Fluids B* **3**, 1059 (1991).